TECHNICAL TRANSACTIONS | **CZASOPISMO TECHNICZNE**
ELECTRICAL ENGINEERING | ELEKTROTECHNIKA
1-E/2015

MAREK CIURYS, IGNACY DUDZIKOWSKI*

ANALYSIS OF A BRUSHLESS DC MOTOR INTEGRATED WITH A HIGH-PRESSURE VANE PUMP

ANALIZA SILNIKA BEZSZCZOTKOWEGO ZINTEGROWANEGO Z WYSOKOCIŚNIENIOWĄ POMPĄ ŁOPATKOWĄ

A b s t r a c t

A new design of a brushless direct current motor is introduced in this paper. In the BLDC motor, a high-pressure vane pump is built into the rotor. The motor is excited by neodymium magnets. Its nominal power is 2.5 kW. The motor is built in such a way that the magnetic field does not penetrate the pump. A magnetic structure field analysis of the motor was performed. Demagnetization resistance of the magnets was determined. By the use of time stepping, finite element method waveforms of the electrical and mechanical parameters in the BLDC motor–inverter system were determined.

Keywords: *electrical machines*, *BLDC motors*, *magnetic structure*, *transients*

S t r e s z c z e n i e

Opracowano nową konstrukcję silnika bezszczotkowego (BLDC), w którego wirnik wbudowana jest wysokociśnieniowa pompa łopatkowa. Silnik wzbudzany magnesami neodymowymi ma moc 2,5 kW. Zbudowany jest w taki sposób, aby pole magnetyczne nie wnikało do wnętrza pompy. Przeprowadzono polową analizę obwodu magnetycznego silnika. Wyznaczono odporność magnesów na odmagnesowanie. Metodą polowo-obwodową wyznaczono przebiegi czasowe wielkości elektrycznych i mechanicznych w układzie silnik–przekształtnik.

Słowa kluczowe: *maszyny elektryczne*, *silniki bezszczotkowe*, *obwód magnetyczny*, *przebiegi czasowe*

DOI: 10.4467/2353737XCT.15.060.3860

* Ph.D. Eng. Marek Ciurys, Prof. D.Sc. Ph.D. Eng. Ignacy Dudzikowski, Faculty of Electrical Engineering, Department of Electrical Machines, Drives and Measurements, Wroclaw University of Technology.

1. Introduction

In existing drive systems with vane pumps, the connection between the pump and the electric motor is usually rendered through an elastic clutch and a mounting flange [2]. This solution is by far the most common [6] in the construction of hydraulic power units. Some simplification of the construction is the direct connection of the pump shaft to the electric motor shaft without a clutch and mounting flange. Such a solution is called a close coupled motor pump group [7]. In all of these solutions, the pump and the motor are two separate components.

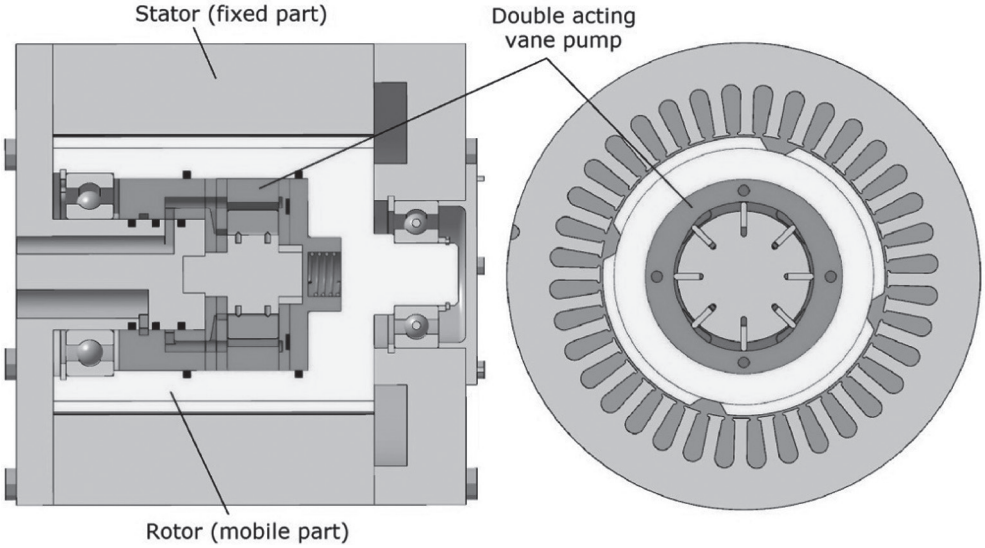

Fig. 1. Design sketch of the double vane pump integrated with the BLDC motor [2]

In this paper, a new design solution for an electrical motor is presented. In this solution (Figs. 1 and 2), the hydraulic pump is built into the rotor of the brushless direct current motor (BLDC motor). This issue has not been analyzed in the available literature.

The stator of the motor is a part of the body of the whole device and the rotor of the electric motor causes rotation of the pump housing. The internal part of the pump (with the vanes) is non-movable. Due to a lack of rotation, the vanes are pressed to the cam ring with spring elements [2].

Electrical drive systems with permanent magnet motors have the highest energy efficiency, the highest power value per unit mass, a large durability and a very good dynamic range [1–5]; therefore, a BLDC motor has been used in the proposed construction of the motor integrated with the vane pump.

The flow of the vane pump is controlled by an electrical motor power converter unit through changing the rotational speed of the motor (by the PWM method). This solution allows the simplification of the hydraulic control systems and reducing the cost of their implementation. The integrated vane pump motor construction has a compact design. The pump is located inside the rotor of the motor, which together with the stator, is an acoustic cover.

Such a solution is therefore characterized by a reduced noise level with respect to the existing, conventional drive systems with vane pumps.

The disadvantage of this solution is the risk of penetration of the magnetic flux into the pump. This could cause the magnetization of metal particles that may be present in the fluid of the hydraulic system. To avoid this, the magnetic structure of the integrated motor-pump construction should be designed in such a way that the magnetic flux does not penetrate the interior of the pump with the liquid.

2. Magnetic structure of the electrical motor

A brushless direct current motor was designed with a power level of P = 2.5 kW at rotational speed n = 3000 rpm and a supply voltage of U = 220 V. High-energy neodymium magnets of N33UH type have been applied. The maximum operating temperature of the magnets is 180°C. The outer diameter of the stator is 135 mm and the packet length is 95 mm.

The required resistance to demagnetization in the heated state (120°C) was provided by permanent magnets with a thickness of 3.5 mm. In order to eliminate the penetration of the magnetic flux into the pump, a non-magnetic sleeve was placed on the outer casing of the pump (Fig. 2).

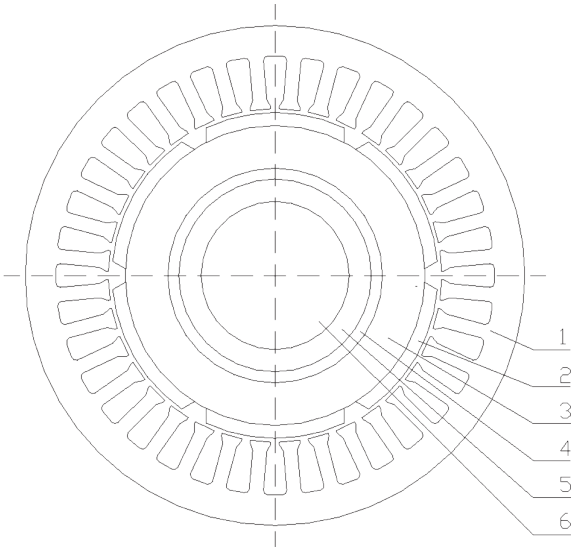

Fig. 2. Cross section of the magnetic structure: 1 – stator sheet, 2 – permanent magnet, 3 – rotor yoke, 4 – non-magnetic sleeve, 5 – casing of the pump, 6 – the interior of the pump (with liquid)

To reduce the size and the weight of stator and rotor, a magnetic structure with 3 pole pairs was used. Computations of the magnetic structure were made by use of Maxwell software. The symmetry of the magnetic circuit was taken into account, hence the computational analysis was performed for the region of one pole pitch.

3. Results of the field computations of the magnetic structure

The aim of the computational analysis was to design a magnetic structure in which the magnetic flux produced by the magnets does not penetrate the interior of the vane pump. To eliminate this phenomenon, a non-magnetic sleeve was applied between the rotor yoke and the casing of the pump (Figs. 2 and 4).

Computational analysis was performed at different values of non-magnetic sleeve thickness. The outer diameter of the pump and the thickness of its steel casing are constant. With changes in the thickness of the non-magnetic sleeve, changes of the rotor yoke thickness occur.

The performed computational analysis shows that the value of the flux density in the interior of the pump is only 13.9 μT when the 3 mm non-magnetic sleeve is applied. This value is smaller than the value of the magnetic field on the surface of the earth (which is approximately 50 μT [8]). Non-magnetic sleeves of a smaller thickness cannot eliminate the phenomenon of the magnetic flux penetration of the interior of the pump.

Due to the fact that the fluid in the hydraulic system can heat up to a temperature of approximately 90°C, the operating temperature of the magnets has been assumed at $\vartheta_m = 120°C$. For the selected 3.5 mm magnet height, the maximum current that does not cause demagnetization is 112 A. This is 6.8 times more than the maximum instantaneous value of the current at steady-state (at the rated load torque). Examples of the computation results are shown in Figs. 3–6.

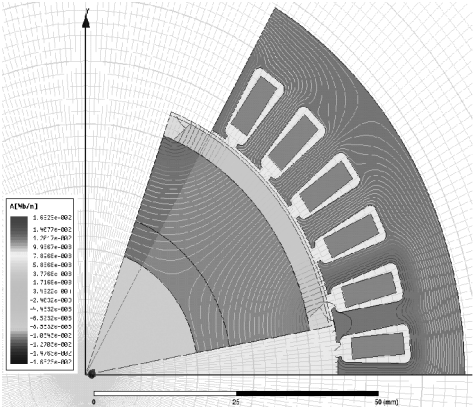

Fig. 3. Flux lines of the motor without the non-magnetic sleeve

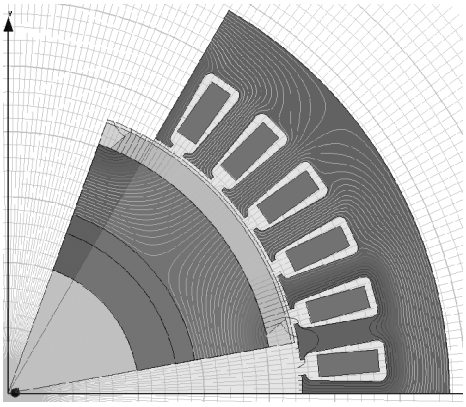

Fig. 4. Flux lines of the motor with the 3 mm non-magnetic sleeve

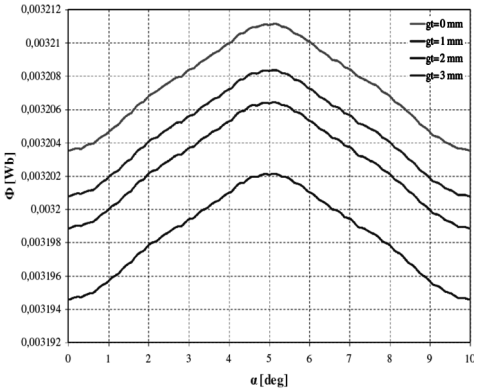

Fig. 5. Magnetic flux versus angle of rotation at different non-magnetic sleeve thicknesses: g_t = 0; 1; 2 and 3 mm

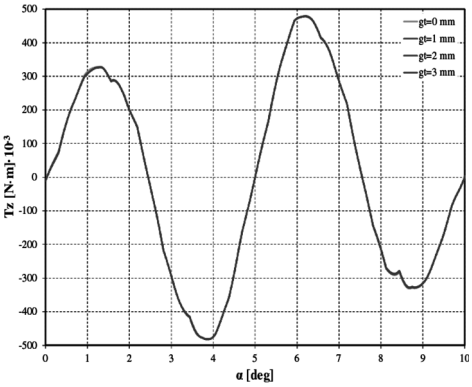

Fig. 6. Cogging torque versus angle of rotation at different non-magnetic sleeve thicknesses: g_t = 0; 1; 2 and 3 mm

4. Field-circuit computations

4.1. Time stepping finite element field-circuit model of the motor with converter

To determine transients of the electrical and mechanical parameters of the designed motor, a time stepping finite element field-circuit model of the motor with a converter was developed in the Maxwell software. The field part of the model is shown in Fig. 3.

The circuit part of the model includes the power supply, the converter and the BLDC motor. The end leakage inductance and resistance of the winding as well as the influence of the temperature on the permanent magnet parameters, the converter diodes and transistors parameters and the armature winding resistance were all considered.

The circuit model of the motor with the converter is shown in Fig. 7, where the symbols stand for: *RA*, *RB*, *RC* – the resistance of the motor winding phases; *EA*, *EB*, *EC* – the summary electromotive force induced in the motor winding phases (including the emf of self and mutual inductance and the emf of rotation). *LAp*, *LBp*, *LCp* are the end leakage inductances of the motor winding phases and *SA*1, *SB*1, *SC*1, *SA*2, *SB*2, *SC*2 stand for transistor switches of the converter; *D*1, …, *D*6 are feedback diodes (model of an ideal *p-n* junction) of the converter, and *R*1, ..., *R*6 are the internal resistances of the converter feedback diodes, V_Uzas is the supply voltage. The circuits with the *VA*, *VB*, *VC*, *VnA*, *VnB*, *VnC*, *RA*1, *RA*2, *RB*1, *RB*2, *RC*1, *RC*2 elements are used to control the transistor switch operation as a function of the rotor position. The resistance of the motor winding phases is 77 mΩ and the end leakage inductance of the motor winding phases is 36 μH.

The main equations of the BLDC motor mathematical model are as follows:

$$u_a = RA_\vartheta \cdot i_a + LA_p \frac{\mathrm{d}i_a}{\mathrm{d}t} + EA(t) \tag{1}$$

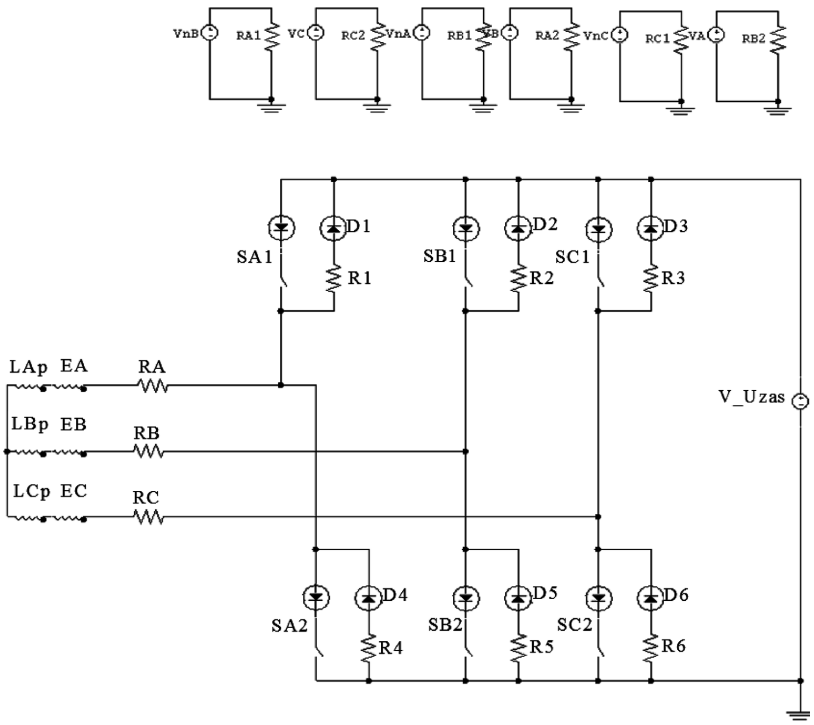

Fig. 7. Circuit model of the BLDC motor with converter

$$u_b = RB_\vartheta \cdot i_b + LB_p \frac{\mathrm{d}i_b}{\mathrm{d}t} + EB(t) \tag{2}$$

$$u_c = RC_\vartheta \cdot i_c + LC_p \frac{\mathrm{d}i_c}{\mathrm{d}t} + EC(t) \tag{3}$$

where:

u_a, u_b, u_c – the instantaneous values of the voltages of *a*, *b* and *c* phases,
RA_ϑ, RB_ϑ, RC_ϑ – the resistance of the armature winding phases at ϑ temperature,
i_a, i_b, i_c – stand for the instantaneous values of the currents in the armature windings of *a*, *b* and *c* phases.

The summary electromotive forces $EA(t)$, $EB(t)$, $EC(t)$ induced in the motor winding phases include the emf of self and mutual inductance and the back emf:

$$EA(t) = L\frac{\mathrm{d}i_a}{\mathrm{d}t} + M\frac{\mathrm{d}i_b}{\mathrm{d}t} + M\frac{\mathrm{d}i_c}{\mathrm{d}t} + e_a \tag{4}$$

$$EB(t) = L\frac{\mathrm{d}i_b}{\mathrm{d}t} + M\frac{\mathrm{d}i_a}{\mathrm{d}t} + M\frac{\mathrm{d}i_c}{\mathrm{d}t} + e_b \tag{5}$$

$$EC(t) = L\frac{\mathrm{d}i_c}{\mathrm{d}t} + M\frac{\mathrm{d}i_a}{\mathrm{d}t} + M\frac{\mathrm{d}i_b}{\mathrm{d}t} + e_c \tag{6}$$

where:

e_a, e_b, e_c – the instantaneous values of back emfs induced in the armature winding phases,
L – the self-inductance of the one armature winding phase (without the end leakage inductance),
M – the mutual inductance of the armature winding phases.

The equation of the currents at the star node of the motor is shown below:

$$i_a + i_b + i_c = 0 \tag{7}$$

The instantaneous value of the electromagnetic torque of the motor equals:

$$T_e(t) = \frac{e_a \cdot i_a + e_b \cdot i_b + e_c \cdot i_c}{\omega} \tag{8}$$

The instantaneous value of the rotor mechanical speed ω is represented in (9):

$$\omega = \frac{\mathrm{d}\alpha}{\mathrm{d}t} \tag{9}$$

where α is the angle of rotation.

The equation of motion for the system is as follows:

$$T_e(t) - T_{tm}(t) - T_o(t) = J\frac{\mathrm{d}\omega}{\mathrm{d}t} + \frac{\omega}{2}\frac{\mathrm{d}J}{\mathrm{d}t} \tag{10}$$

where:

T_o(t) – the instantaneous value of the load torque,
J – moment of inertia of the motor with the rotating part of the vane pump,
$T_{tm}(t)$ – stands for the instantaneous value of friction torque of the motor:

$$T_{tm}(t) = \frac{\Delta P_m(\omega)}{\omega} \tag{11}$$

where $\Delta P_m(\omega)$ are the windage and friction loss as the function of ω speed.

For the analysed drive system, $\frac{\mathrm{d}J}{\mathrm{d}t} = 0$, hence the equation of motion is as follows:

$$T_e(t) - T_{tm}(t) - T_o(t) = J\frac{\mathrm{d}\omega}{\mathrm{d}t} \tag{12}$$

The instantaneous value of the mechanical torque of the motor is:

$$T(t) = T_e(t) - T_{tm}(t) \tag{13}$$

4.2. Results of the time stepping finite-element computations

For the final motor magnetic structure (with the 3 mm non-magnetic sleeve), waveforms of the electrical and mechanical parameters of the motor have been computed. The computations have been performed for the system with the motor current limit at the value of 4 I_{max}, where I_{max} is the maximum value of the phase current at the steady state at the nominal load torque. Examples of the computation results obtained at the nominal load torque (T_o = 7.96 N·m) are shown in Figs. 8–16.

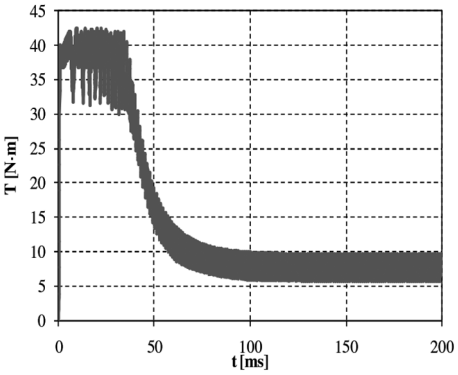

Fig. 8. Transient of the motor mechanical torque at the start-up

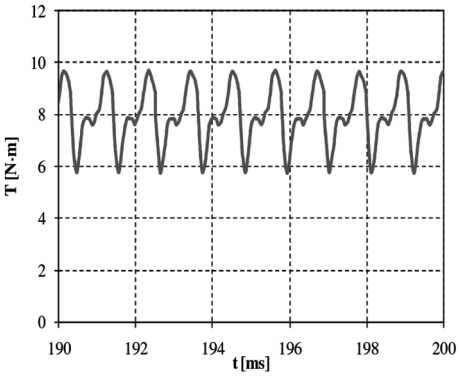

Fig. 9. Mechanical torque of the motor at the steady state

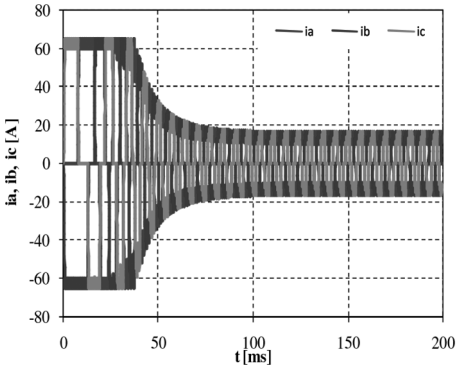

Fig. 10. Waveforms of the phases currents at the motor start-up

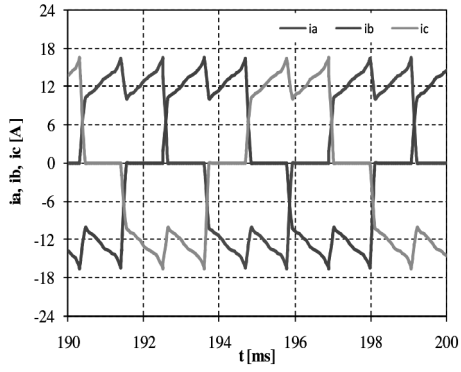

Fig. 11. Waveforms of the phases currents at the steady state

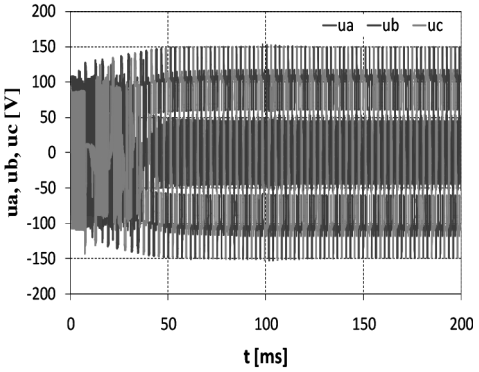

Fig. 12. Waveforms of the phases voltages at the motor start-up

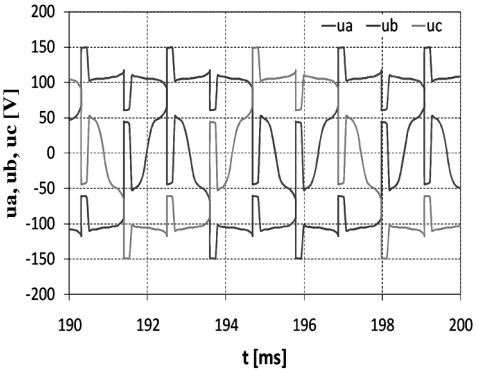

Fig. 13. Waveforms of the phases voltages at the steady state

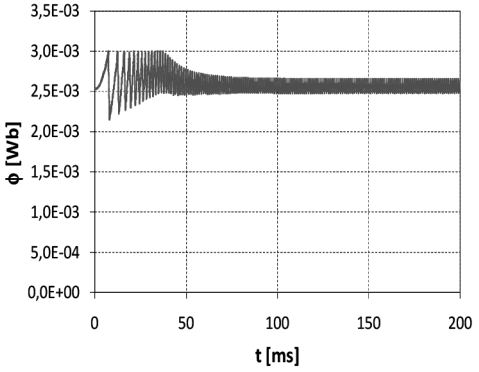

Fig. 14. Magnetic flux in the air-gap at the motor start-up

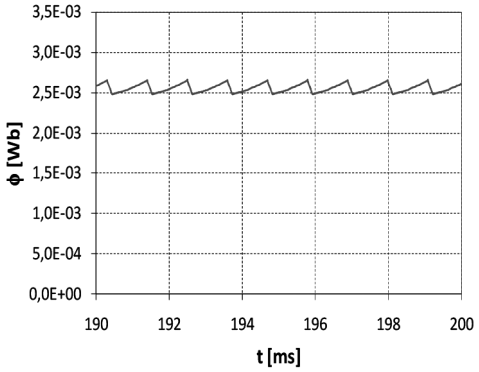

Fig. 15. Magnetic flux in the air-gap at the steady state

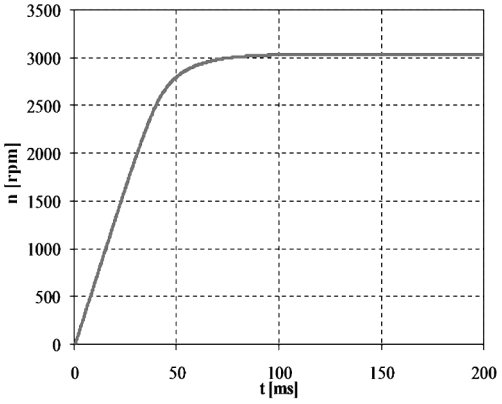

Fig. 16. Rotational speed at the motor start-up

5. Conclusion

A new design for a permanent magnet motor has been reported in this paper. In this motor, a high-pressure vane pump is built into the rotor. In order to eliminate the phenomenon of magnetic flux penetration through the pump, a non-magnetic sleeve was used in the rotor of the electric motor (on the outer steel casing of the pump).

FEM computations of the motor magnetic structure at different non-magnetic sleeve thicknesses were performed. The computational analysis has shown that the non-magnetic sleeve of 3 mm is the best solution. For this thickness, the value of the flux density in the outer steel casing of the pump is 11 mT. It provides a bypass for the magnetic flux and protects against penetration of the magnetic flux into the interior (with liquid) of the pump. The value of the flux density in the interior of the pump is only 13.9 μT. This value is smaller than the value of the magnetic field on the surface of the earth, which is approximately 50 μT [8]. Such a small value of flux density in the liquid of the pump eliminates the danger of magnetization of the metallic particles that may be present in the liquid due to wear of the hydraulic system components.

The decrease of the magnetic flux value in the developed magnetic structure with the non-magnetic 3 mm sleeve is approximately 0.3%. The rise of the temperature of the magnets from 20°C to 120°C causes more than a 3.5-fold decrease of their demagnetization resistance. This confirms that the resistance to demagnetization should be analysed at the highest operating temperature.

Waveforms of the electrical and mechanical parameters of the motor have been computed for the final magnetic structure (with the non-magnetic 3 mm sleeve). The computations have been performed for the system with the motor current limit at a value of 4 I_{max}, where I_{max} is the maximum value of the phase current at the steady-state, at the nominal load torque. The preliminary analysis has shown that the mass of the integrated electrical motor pump system is about 40% smaller than the mass of the conventional solution with the separate pump and motor which are presented, for example, in [2, 6, 7].

References

[1] Dudzikowski I., Ciurys M., *Commutator and brushless motors excited by permanent magnets*, Publishing House of the Wroclaw University of Technology, Wroclaw 2011.
[2] Fiebig W., Dudzikowski I., Ciurys M., Kuczwara H., *Vane Pump integrated into an Electric Motor*, The 9th International Fluid Power Conference, 9 IFK, March 24–26, 2014, Aachen, Germany.
[3] Gieras J.F., *Advancements in Electric Machines*, Springer 2008.
[4] Gieras J.F., Wing M., *Permanent Magnet Motor Technology*, Marcel Dekker, Inc., New York–Basel 2002.
[5] Glinka T., *Permanent magnet electrical machines*, Publishing House of the Silesian University of Technology, Gliwice 2002.
[6] Stryczek S., *Hydrostatic drive*, Vols. 1, 2, WNT, Warsaw 1993.
[7] *Parker Hannifin catalog*.
[8] *Moon and distant quasars facilitate first measurement of magnetic field in Earth's core*, University of California, Berkeley (published: Monday, December 20, 2010).

This work has been financed by The Polish National Centre for Research and Development, project number 208471.